

Angle-resolved photoemission study of the strongly correlated semiconductor FeSi

M. Arita,¹ K. Shimada,¹ Y. Takeda,² M. Nakatake,¹ H. Namatame,¹ M. Taniguchi,^{1,3} H. Negishi,⁴ T. Oguchi,⁴ T. Saitoh,⁵ A. Fujimori,⁶ and T. Kanomata⁷

¹Hiroshima Synchrotron Radiation Center, Hiroshima University, Higashi-Hiroshima 739-0046, Japan

²Synchrotron Radiation Research Unit, Japan Atomic Energy Agency, SPring-8, Sayo, Hyogo 679-5148, Japan

³Graduate School of Science, Hiroshima University, Higashi-Hiroshima 739-8526, Japan

⁴Department of Quantum Matter, ADSM, Hiroshima University, Higashi-Hiroshima 739-8530, Japan

⁵Department of Applied Physics, Tokyo University of Science, Shinjuku-ku, Tokyo 162-8601, Japan

⁶Department of Complexity Science and Engineering, University of Tokyo, Chiba 277-8561, Japan

⁷Faculty of Engineering, Tohoku Gakuin University, Tagajo, Miyagi 985-8537, Japan

(Received 18 February 2008; revised manuscript received 11 April 2008; published 20 May 2008)

The temperature-dependent electronic states of FeSi have been studied by using high-resolution angle-resolved photoemission spectroscopy (ARPES) and using low-energy tunable photons. At low temperatures, a peak indicating the valence-band maximum (VBM) exists at a binding energy of ~ 20 meV along the ΓR direction. The observed dispersional width of the energy bands is narrower than that given by the band-structure calculation, and the width of the ARPES peak near the VBM rapidly broadens as the binding energy increases. Analysis of a model self-energy reveals the importance of electron correlation, especially near the VBM. We observed an unusual temperature dependence of the ARPES spectral features near the Fermi level (E_F): Below ~ 100 K, the peak at the VBM and the energy gap structures are almost unchanged, while at ~ 100 – 350 K, the peak gradually moves toward E_F and the gap is filled. The present results indicate that FeSi is a strongly correlated semiconductor, with a renormalized band near E_F being responsible for the rapid collapse of the peak and the coherent energy gap upon heating.

DOI: [10.1103/PhysRevB.77.205117](https://doi.org/10.1103/PhysRevB.77.205117)

PACS number(s): 71.30.+h, 71.20.Lp, 71.28.+d, 79.60.-i

For more than 40 years, FeSi has attracted many researchers for its anomalous electrical and magnetic properties.^{1–14} From band-structure calculations, FeSi is considered to be a nonmagnetic band insulator with an energy gap of $E_g^{LDA} \sim 100$ meV.^{11–13} Below ~ 100 K, the temperature dependence of the electronic resistivity shows an insulating behavior. However, this gradually changes upon heating and becomes metallic above ~ 300 K.^{2–5} As the temperature increases, the magnetic susceptibility starts to rise at ~ 100 K and forms a broad maximum at ~ 500 K, above which it decreases following the Curie-Weiss law.^{1–10} These behaviors cannot be explained by the simple band model. Jaccarino *et al.*¹ tried to explain the temperature variance of the magnetic susceptibility by assuming that there were localized levels near the Fermi level (E_F). This phenomena has also been explained by the spin-fluctuation theory, taking into account a narrow gap in the electronic density of states (DOS).¹⁵ Recently, interest in FeSi has been revived since the physical properties are claimed to be similar to those of the $4f$ -electron Kondo insulators,¹⁶ which are potential candidates for new thermoelectric materials.¹⁷ The temperature-dependent optical measurements of FeSi show a rapid collapse of the energy gap and an unusual spectral weight transfer from $\omega \sim 0$ to an energy range much larger than the energy gap.¹⁴ This unusual temperature dependence may result from electron correlation.¹⁴

Photoemission spectroscopy is a powerful method to directly examine the electronic states of solids. To date, angle-integrated photoemission spectroscopy (AIPES) studies using a helium lamp ($h\nu = 21.2$ eV and 40.8 eV) have revealed that in the binding energy range of $E_B \sim 0$ – 50 meV, the DOS is suppressed upon cooling.^{18–21} However, the residual

spectral intensity is high at E_F , which is thought to be caused by the metallic states at the surface.²⁰ Recently, a high-resolution AIPES study using a laser ($h\nu = 6.994$ eV) has been carried out.²² Due to the long inelastic mean free path of a photoelectron with a kinetic energy $E_K \lesssim 10$ eV, one can probe bulk-derived electronic states. The residual spectral intensity at E_F was found to be reduced, which suggests that most of the spectral intensity at E_F taken at $h\nu \gtrsim 20$ eV is derived from the metallic state at the surface. As for the band-structure, Park *et al.*²³ performed angle-resolved photoemission spectroscopy (ARPES) on a cleaved FeSi(100) at $h\nu = 24$ eV and observed a sharp peak that forms the valence band maximum (VBM) in the $\Gamma X M \Gamma$ plane of the Brillouin zone (BZ). The peak width significantly increased with increasing E_B ; the peak was not clearly detected for $E_B \gtrsim 30$ meV. Furthermore, the peak intensity was strongly enhanced upon cooling. Hinarejos *et al.*²⁴ prepared a FeSi (111) thin film on Si (111) and performed ARPES at room temperature. It was found that the observed band structures in the wide-binding energy range along the ΓR direction are in agreement with a band-structure calculation. However, the energy dependence of the self-energy derived from the electron-electron interaction has not been explicitly clarified as yet, and the bulk-derived ARPES spectral features close to the VBM still have not been explained as a function of temperature.

In this paper, by means of high-resolution low-excitation energy ARPES, we have proved that the renormalized band exists at the VBM and that, therefore, FeSi is a strongly correlated semiconductor. We discuss the unusual temperature dependence of the ARPES spectral features from the viewpoint of the collapse of the coherent energy gap due to a strong correlation among thermally induced carriers near E_F .

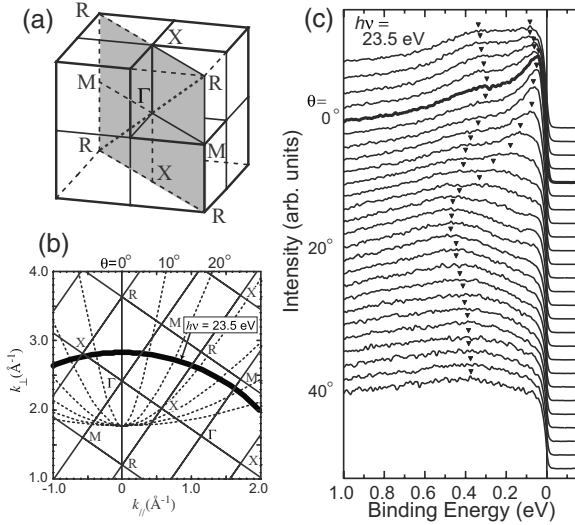


FIG. 1. (a) Brillouin zone of FeSi. The Γ XRM plane (gray) was measured by ARPES experiment. (b) Relation between k_{\perp} and k_{\parallel} . The solid curve shows the cross-section of the Brillouin zone measured by the ARPES with $h\nu=23.5$ eV. (c) ARPES spectra of FeSi taken at $h\nu=23.5$ eV. Structures are indicated by triangles.

High-energy-resolution ARPES measurements were conducted with tunable low-energy photons on the helical undulator beamline BL-9A of the compact electron-storage ring (HiSOR) at Hiroshima Synchrotron Radiation Center, Hiroshima University.²⁵ A high-resolution hemispherical electron-energy analyzer SES2002 (Gammadata-Scientia, Sweden) was used. The total energy resolution, including for both the electron-energy analyzer and the monochromator, was set at $\Delta E=1.3$ – 8 meV at $h\nu=5.48$ – 23.5 eV. The base pressure of the chamber was 1×10^{-8} Pa.

The FeSi single crystal samples were synthesized according to the Czochralski method.^{6,7} The lattice constant was determined to be $a=4.4853$ Å.⁷ From the magnetic susceptibility measurements, the energy gap was estimated to be $E_g=62$ meV.⁶ On the basis of the extrinsic paramagnetic component below ~ 80 K, and assuming that the impurity ion is Fe^{+3} ($S=5/2$), the impurity concentration was evaluated to be 0.1% of the concentration of Fe,⁶ or 4.1×10^{19} cm⁻³.⁷ The FeSi single crystal was shaped into parallelepiped rods by using Laue photographs and the (111) surface was positioned toward the analyzer in the normal emission geometry. The clean surfaces were obtained by cleaving with a knife edge *in-situ*.²⁶ A sharp peak feature near the VBM and dispersive bands in the wide energy range were clearly observed. The position of E_F was determined by referring to the Fermi edge of the Au film electrically connected to the sample before and after data accumulation.

In the ARPES experiments, the sample was rotated around the $[1\bar{1}0]$ axis. The rotation angle θ was measured from the $[111]$ direction toward $[11\bar{2}]$ ($[110]$). With this geometry, energy bands in the Γ XRM plane of the BZ were detected [gray plane in Fig. 1(a)]. At $h\nu=23.5$ eV, one could examine the cross section of the Fermi surface in the Γ XRM plane as indicated by the solid curve in Fig. 1(b). It was assumed that the inner potential and the work function were

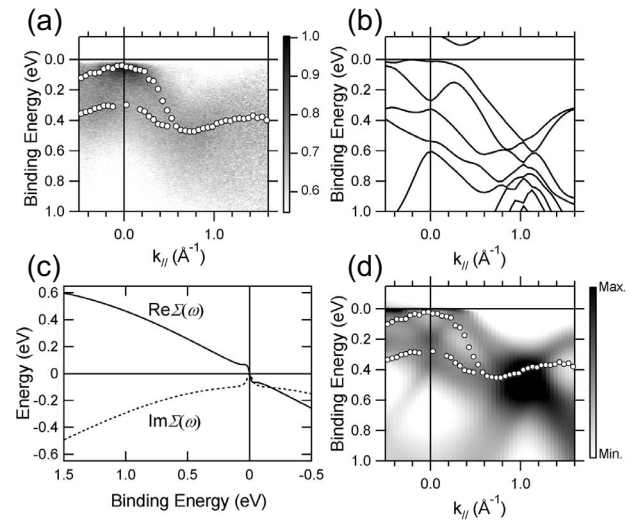


FIG. 2. (a) Intensity plot of the ARPES spectra. The open circles indicate the peak positions. (b) Calculated LSDA band structures along the solid line in Fig. 1(b). (c) Real and imaginary parts of $\Sigma(\omega)$ assumed in the present analyses. (d) Intensity map of $A(\mathbf{k}, \omega)$ with the self-energy correction. A Gaussian function with a width of 5 meV FWHM was convoluted to represent energy resolution.

12 eV and 4.5 eV, respectively. Figure 1(c) shows the ARPES spectra taken at $h\nu=23.5$ eV at 20 K with a momentum resolution of $\Delta k=0.01$ Å⁻¹. A peak structure was observed at $\theta=0^\circ$ at $E_B \sim 40$ meV that moves toward higher binding energies with $|\theta|$. One can recognize that the peak disperses until $E_B \sim 500$ meV. The peak becomes sharper as it approaches E_F .

Figure 2(a) represents an intensity plot on a linear grayscale in E_B - k_{\parallel} plane. The open circles indicate the positions of the structures in the ARPES spectra and show band dispersions. The band is closest to E_F around $k_{\parallel}=0$ Å⁻¹, which suggests that the VBM is located on the Γ -R line. Figure 2(b) shows the band structures along the solid curve in Fig. 1(b), which was calculated by using the full potential linearized augmented plane wave method (FLAPW). The calculated energy gap is $E_g^{LDA} \sim 100$ meV. There exist bands close to E_F around $k_{\parallel}=0$ Å⁻¹, which disperse to $E_B \sim 600$ meV at $k_{\parallel} \sim 1$ Å⁻¹, which are in qualitative agreement with the observed band structures. However, the observed dispersional bandwidth, which is ~ 500 meV, is slightly narrower than the calculated one, ~ 600 meV. Furthermore, the peak that forms the VBM is quickly broadened as it shifts away from E_F because of a change in $|\theta|$. It is also difficult to identify the peak for $E_B \geq 50$ meV, which is in agreement with previous ARPES measurements.²³

Figure 3(a) shows the normal emission ARPES spectra at 5 K. Here, the acceptance angle of the analyzer was set at $\theta = \pm 5^\circ$ [$\Delta k=0.1$ – 0.3 Å⁻¹, indicated by a dashed line in Fig. 3(b)]. For $h\nu=7$ – 10 eV, peaks were clearly observed near E_F only around the normal emission (i.e., $[111]$) direction. The peak shifted to higher E_B above and below $h\nu=8.4$ eV. Figures 3(b) and 3(c) show measured \mathbf{k} points in the BZ by means of normal emission ARPES ($h\nu=5.48$ eV– 14.8 eV) along the Γ R line and the energy bands calculated within the local-density approximation (LDA)

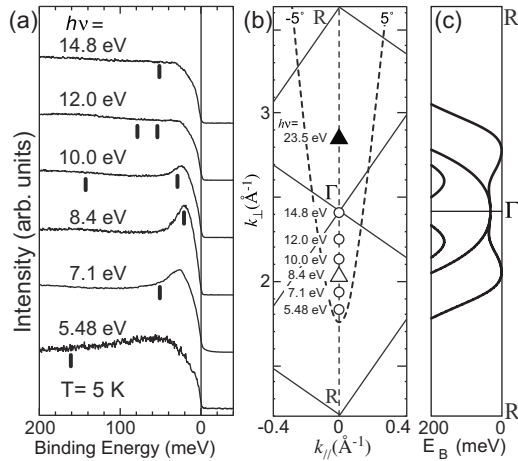


FIG. 3. (a) Normal emission ARPES spectra at 5 K. The vertical bars show the energy positions given by the LDA calculation. The energy position of the calculated VBM has been adjusted to coincide with the observed VBM. (b) Measured k points in the BZ by means of normal emission ARPES. (c) Band structure given by the LDA calculation along the ΓR line.

along the ΓR line, respectively. The ARPES spectra taken at $h\nu=23.5$ eV and 8.4 eV correspond to almost the same \mathbf{k} point in the BZ and the observed peak positions are in agreement with the calculated VBM positions. However, the observed peak positions away from the VBM have lower E_B than the calculated ones [bars in Fig. 3(a)]. The normal emission ARPES results also suggest that the peak becomes narrower as it approaches E_F , which is in agreement with the $|\theta|$ scan taken at $h\nu=23.5$ eV [Fig. 1(c)]. These results are highly suggestive of strong renormalization, especially near the VBM.

ARPES spectral features are represented by the single-particle spectral function: $A(\mathbf{k}, \omega) = -\frac{1}{\pi} \text{Im} \frac{1}{\omega - \epsilon_{\mathbf{k}}^0 - \Sigma(\mathbf{k}, \omega)}$. Here, $\Sigma(\mathbf{k}, \omega)$ is derived from many-body interactions, such as the electron-electron and the electron-phonon interactions.²⁷ The imaginary part of the self-energy is related to the energy-dependent peak-width broadening, $\Gamma = 2|\text{Im}\Sigma(\mathbf{k}, \omega)|$. The real part of the self-energy corresponds to the energy shift from the noninteraction band: $\text{Re}\Sigma(\mathbf{k}, \omega) = \omega_{\mathbf{k}} - \epsilon_{\mathbf{k}}^0$.

On the basis of the observed band narrowing in the wide energy range and significant peak-width broadening near the VBM, we have assumed that the deviation from the LDA calculation is mainly derived from electron correlation.

In order to demonstrate the renormalization effect derived from the electron-electron interaction, a simple analytic function introduced by Saitoh *et al.*¹⁹ was adopted. They calculated the spectral function by assuming a k -independent analytical self-energy $\Sigma(\omega) = \Sigma_h(\omega) + \Sigma_l(\omega)$, where $\Sigma_h(\omega) = g_h \omega / (\omega + i\gamma_h)^2$ and $\Sigma_l(\omega) = -g_l / (\omega + i\gamma_l) - i g_l / \gamma_l$.¹⁹ It should be noted that this model includes the self-energy for the low energy region, $\Sigma_l(\omega)$, which represents the strong renormalization near the VBM. The real and the imaginary parts are shown in Fig. 2(c); the parameters used in the previous study were $g_h = 13.0$, $\gamma_h = 5.0$, $g_l = 0.0025$ and $\gamma_l = 0.025$.¹⁹

Figure 2(d) exhibits an intensity map of $A(\mathbf{k}, \omega)$ that was calculated by using the parameters previously used. The open circles indicate the observed band positions. Although

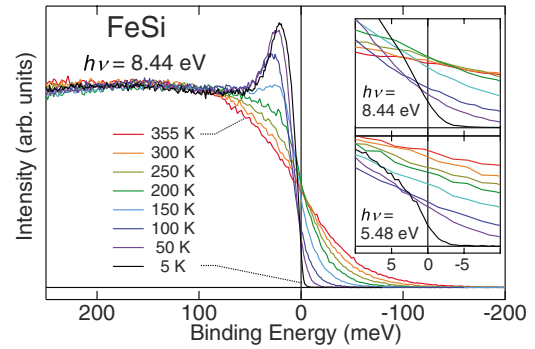


FIG. 4. (Color online) Temperature-dependent spectra at $h\nu = 8.44$ eV. The inset shows the spectra close to E_F for $h\nu = 8.44$ and 5.48 eV.

we did not optimize these parameters, this simulation was found to reasonably explain experimental results. The band width is narrowed by $(1 - \partial \text{Re}\Sigma / \partial \omega)^{-1} \sim 0.7$ in the wide energy range, which explains the reduction of the energy gap $E_g / E_g^{LDA} \sim 0.6$. A broad spectral structure at $E_B \sim 500$ meV at $k_{\parallel} \sim 1 \text{ \AA}^{-1}$ was reproduced with the model self-energy. We should note that the substantial energy dependence of the peak width near the VBM could not be explained without $\Sigma_l(\omega)$ for $|\omega| \lesssim 0.025$. This supports the hypothesis that the renormalization due to the electron-electron interaction is more significant near the VBM.²⁸

We then examined the temperature dependence of the peak structure at the VBM. The peak was most significantly enhanced and closest to E_F ($E_B = 20$ meV) in the spectrum taken at $h\nu = 8.44$ eV at 5 K. Figure 4 shows the temperature dependence of the 8.44 eV spectra. The spectra have been normalized to the intensity integrated between $E_B = -200$ meV and 200 meV. Although the intensity of the peak observed at 5 K considerably decreases with increasing temperature, the intensity for $E_B > 150$ meV did not change. Therefore, the significant temperature variation only occurs within a narrow energy range near the VBM. This coincides with the fact that the significantly renormalized band exists near the VBM. The spectral intensity taken at various temperatures is conserved within $|E_B| < 200$ meV, which is consistent with the previous AIPES experiments.²² The inset of Fig. 4 shows that the bulk-sensitive photoemission spectra taken at $h\nu = 5.48$ and 8.44 eV have finite residual intensity at E_F , which is similar to a previous AIPES result.²² The residual intensity is assumed to originate from impuritylike states (or a many-body resonance²⁹), which are responsible for an anomalous metallic conductivity below ~ 1 K,^{3,4} an anomalous Hall effect,^{3,29} and a complicated magnetic phase diagram below 20 K.²⁹

In order to evaluate the experimental $A(\mathbf{k}, \omega)$ near the VBM, the 8.44 eV spectra taken at various temperatures were divided by the Fermi-Dirac distribution function convoluted with a Gaussian function that represents energy resolution as shown in Fig. 5(a). Spectral weight above E_F can be observed within $E_B \sim -5k_B T \sim -100$ meV at 150–200 K.³⁰ Since a peak was not observed on the unoccupied side, the energy gap should be indirect as predicted by the LDA calculations.^{11,12} The peak width broadens as the temperature

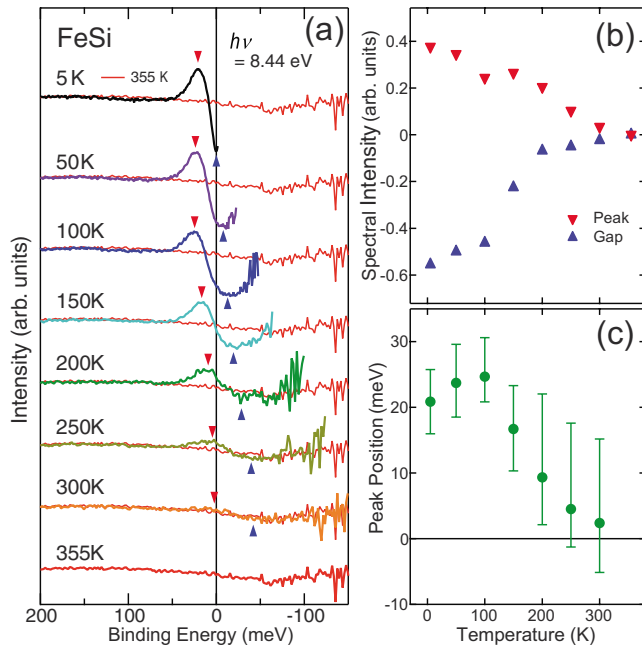


FIG. 5. (Color online) Temperature-dependence of photoemission spectra at 8.44 eV in normal emission. (a) Experimental $A(\mathbf{k}, \omega)$. The positions of the peak and the gap are indicated by triangles. (b) Temperature dependence of the peak and gap intensity. (c) Peak position as a function of temperature.

increases. At 355 K, one cannot see the energy gap in the observed $A(\mathbf{k}, \omega)$.

Figure 5(b) shows the spectral intensity at the peak and at the gap as a function of temperature. Upon heating, the peak intensity decreases. The gap starts to decrease above ~ 100 K, and almost disappears at ~ 300 K.

Figure 5(c) exhibits that the peak position is almost unchanged below ~ 100 K. From 100 to 150 K, however, the peak was significantly shifted toward lower E_B , and the energy gap completely disappeared at ~ 355 K.

These observations are consistent with the temperature dependences of the electrical resistivity^{2–5} and the magnetic susceptibility.^{6,7,31} On the basis of the ARPES results, we have tried to describe the temperature-dependent electronic states of FeSi. Since there are no structural and magnetic phase transitions above 50 K,^{32,33} electron correlation should play a principal role in the unusual temperature dependence. Electron correlation in FeSi has been theoretically explained by using the spin-fluctuation theory,¹⁵ LDA+U,³⁴ the Anderson lattice model,³⁵ and the two-band Hubbard model.^{36,37} For the temperature region $T \leq 100$ K, the electrons and holes cannot be thermally excited due to the existence of the energy gap. The impuritylike states near E_F affect the physi-

cal properties. The binding energies of the observed band are, however, smaller than those given by the LDA calculation. Furthermore, there exists a noticeable energy-dependent peak-width broadening, especially near the VBM. The simulation with the model self-energy, taking into account strong renormalization near the VBM, reproduced our ARPES results. These results indicate that FeSi is not an ordinary semiconductor but a strongly correlated one.

The electron correlation effect manifests itself as the temperature increases. For the temperature region $100 \text{ K} \leq T \leq 350 \text{ K}$, a peak shift toward E_F and a peak-width broadening take place. The energy gap gradually disappears upon heating. It is interesting to note that these unusual behaviors are similar to the temperature-dependence of the energy gap of the *f*-electron Kondo semiconductors.^{16,38,39} We assume that above ~ 100 K the electron correlation effects among the temperature-induced carriers become significant. Namely, the increase of the inelastic scattering among carriers upon heating accelerates the collapse of the energy gap. The energy range for the significantly renormalized band near the VBM is ~ 50 meV, which is in accord with the fact that an obvious temperature variance of the spectral features is observed in the narrow energy range near E_F . The rapid temperature-dependent collapse of the energy gap due to electron correlation is described by the two-band Hubbard model calculation.³⁷

For the temperature region $T \geq 350$ K, no peak and gap structures exist around E_F , which is in agreement with the metallic behavior. It is to be noted that at elevated temperatures the spin-fluctuation effect is important in explaining the unusual magnetic properties of FeSi.¹⁵

In summary, high-resolution ARPES measurements of FeSi single crystals have been performed with tunable low-energy photons. We have observed a peak at ~ 20 meV that forms the VBM along the ΓR direction. We have clarified that there exists strong renormalization near the VBM. The temperature dependence of the spectra indicates that the significant temperature variation occurs in a narrow energy range around the VBM and the energy gap in the experimental $A(\mathbf{k}, \omega)$ rapidly collapses above ~ 100 K. The present results illustrate that electron correlation plays an important role in the metal-insulator transition in FeSi and, thus, FeSi can be considered a strongly correlated semiconductor.

This work was partly supported by a Grant-in-Aid for the Scientific Research (Grant No. 17654060) of MEXT, Japan. We thank the Materials Science Center, N-BARD, Hiroshima University for supplying liquid helium. The synchrotron radiation experiments were done with the approval of HSRC (Proposal No. A01–28).

¹V. Jaccarino, G. K. Wertheim, J. H. Wernick, L. R. Walker, and S. Araj, Phys. Rev. **160**, 476 (1967).

²M. B. Hunt, M. A. Chernikov, E. Felder, H. R. Ott, Z. Fisk, and P. Canfield, Phys. Rev. B **50**, 14933 (1994).

³S. Paschen, E. Felder, M. A. Chernikov, L. Degiorgi, H. Schwer, H. R. Ott, D. P. Young, J. L. Sarrao, and Z. Fisk, Phys. Rev. B **56**, 12916 (1997).

⁴M. Fäth, J. Aarts, A. A. Menovsky, G. J. Nieuwenhuys, and J. A.

- Mydosh, Phys. Rev. B **58**, 15483 (1998).
- ⁵R. Wolfe, J. H. Wernick, and S. E. Haszko, Phys. Lett. **19**, 449 (1965).
- ⁶K. Koyama, T. Goto, T. Kanomata, and R. Note, J. Phys. Soc. Jpn. **68**, 1693 (1999).
- ⁷K. Koyama, T. Goto, T. Kanomata, R. Note, and Y. Takahashi, J. Phys. Soc. Jpn. **69**, 219 (2000).
- ⁸M. Imada, A. Fujimori, and Y. Tokura, Rev. Mod. Phys. **70**, 1039 (1998).
- ⁹S. Takagi, H. Yasuoka, S. Ogawa, and J. H. Wernick, J. Phys. Soc. Jpn. **50**, 2539 (1981).
- ¹⁰M. Corti, S. Aldrovandi, M. Fanciulli, and F. Tabak, Phys. Rev. B **67**, 172408 (2003).
- ¹¹L. F. Mattheiss and D. R. Hamann, Phys. Rev. B **47**, 13114 (1993).
- ¹²T. Arioka, E. Kulatov, H. Ohta, S. Halilov, and L. Vinokurova, Physica B (Amsterdam) **246-247**, 541 (1998).
- ¹³T. Jarlborg, Phys. Rev. B **59**, 15002 (1999).
- ¹⁴Z. Schlesinger, Z. Fisk, H.-T. Zhang, M. B. Maple, J. F. DiTusa, and G. Aeppli, Phys. Rev. Lett. **71**, 1748 (1993).
- ¹⁵T. Moriya and Y. Takahashi, J. Phys. Soc. Jpn. **45**, 397 (1978); Y. Takahashi and T. Moriya, *ibid.* **46**, 1451 (1979); Y. Takahashi, J. Phys.: Condens. Matter **9**, 2593 (1997); Y. Takahashi, *ibid.* **10**, L671 (1998); Y. Takahashi, T. Kanomata, R. Note, and T. Nakagawa, J. Phys. Soc. Jpn. **69**, 4018 (2000).
- ¹⁶G. Aeppli and Z. Fisk, Comments Condens. Matter Phys. **16**, 155 (1992).
- ¹⁷G. D. Mahan and J. O. Sofo, Proc. Natl. Acad. Sci. U.S.A. **93**, 7436 (1996).
- ¹⁸A. Chainani, T. Yokoya, T. Morimoto, T. Takahashi, S. Yoshii, and M. Kasaya, Phys. Rev. B **50**, 8915 (1994).
- ¹⁹T. Saitoh, A. Sekiyama, T. Mizokawa, A. Fujimori, K. Ito, H. Nakamura, and M. Shiga, Solid State Commun. **95**, 307 (1995).
- ²⁰K. Breuer, S. Messerli, D. Purdie, M. Garnier, M. Hengsberger, Y. Baer, and M. Mihalik, Phys. Rev. B **56**, R7061 (1997).
- ²¹T. Susaki, T. Mizokawa, A. Fujimori, A. Ohno, T. Tonogai, and H. Takagi, Phys. Rev. B **58**, 1197 (1998).
- ²²K. Ishizaka, T. Kiss, T. Shimojima, T. Yokoya, T. Togashi, S. Watanabe, C. Q. Zhang, C. T. Chen, Y. Onose, Y. Tokura, and S. Shin, Phys. Rev. B **72**, 233202 (2005).
- ²³C. H. Park, Z. X. Shen, A. G. Loeser, D. S. Dessau, D. G. Mandrus, A. Migliori, J. Sarrao, and Z. Fisk, Phys. Rev. B **52**, R16981 (1995).
- ²⁴J. J. Hinarejos, P. Segovia, J. Alvarez, G. R. Castro, E. G. Michel, and R. Miranda, Phys. Rev. B **57**, 1414 (1998).
- ²⁵M. Arita, K. Shimada, H. Namatame, and M. Taniguchi, Surf. Rev. Lett. **9**, 535 (2002).
- ²⁶We cleaved single crystalline FeSi samples many times and confirmed the reproducibilities of the spectral features. Especially, the spectral features of the peak at $E_B \sim 20$ meV taken at $h\nu \sim 8.4$ eV were reproduced many times. The peak was not observed for the cleaved surface of the polycrystalline sample or the scraped surface of a single crystalline sample.
- ²⁷S. Hüfner, *Photoelectron Spectroscopy*, 3rd ed. (Springer-Verlag, Berlin, 2003), Chap. 1, and references therein.
- ²⁸The scattering due to the defects or disorders of the cleaved surface should be regarded as due to the electron-impurity scattering, which gives the energy-independent peak-width broadening of the ARPES spectra. The energy dependent peak-width broadening, therefore, should be ascribed to the intrinsic scattering, i.e., the electron-electron scattering.
- ²⁹N. Sluchanko, V. Glushkov, S. Demishev, M. Kondrin, V. Ivanov, K. Petukhov, N. Samarin, A. Menovsky, and V. Moshchalkov, JETP **92**, 312 (2001); V. V. Glushkov, I. B. Voskobonikov, S. V. Demishev, I. V. Krivitskii, A. Menovsky, V. V. Moshchalkov, N. A. Samarin, and N. E. Sluchanko, *ibid.* **99**, 312 (2004); N. E. Sluchanko, V. V. Glushkov, S. V. Demishev, M. V. Kondrin, K. M. Petukhov, N. A. Samarin, V. V. Moshchalkov, and A. A. Menovsky, Europhys. Lett. **51**, 557 (2000).
- ³⁰T. Greber, T. J. Kreuz, and J. Osterwalder, Phys. Rev. Lett. **79**, 4465 (1997).
- ³¹E. Arushanov, M. Respaud, J. M. Broto, J. Leotin, S. Askenazy, C. Kloc, E. Bucher, and K. Lisunov, Phys. Rev. B **55**, 8056 (1997).
- ³²L. Vočadlo, K. S. Knight, G. D. Price, and I. G. Wood, Phys. Chem. Miner. **29**, 132 (2002).
- ³³H. Watanabe, H. Yamamoto, and I. Ken-ichi, J. Phys. Soc. Jpn. **18**, 995 (1963).
- ³⁴V. I. Anisimov, S. Y. Ezhov, I. S. Elfimov, I. V. Solovyev, and T. M. Rice, Phys. Rev. Lett. **76**, 1735 (1996).
- ³⁵P. S. Riseborough, Phys. Rev. B **58**, 15534 (1998).
- ³⁶C. Fu and S. Doniach, Phys. Rev. B **51**, 17439 (1995).
- ³⁷K. Urasaki and T. Saso, Phys. Rev. B **58**, 15528 (1998); K. Urasaki and T. Saso, J. Phys. Soc. Jpn. **68**, 3477 (1999).
- ³⁸Y. Takeda, M. Arita, M. Higashiguchi, K. Shimada, H. Namatame, M. Taniguchi, F. Iga, and T. Takabatake, Phys. Rev. B **73**, 033202 (2006), and references therein.
- ³⁹K. Shimada, in *Very High Resolution Photoelectron Spectroscopy*, Lecture Notes in Physics Vol. 715, edited by S. Hüfner (Springer-Verlag, Berlin, 2007), Chap. 4, and references therein.